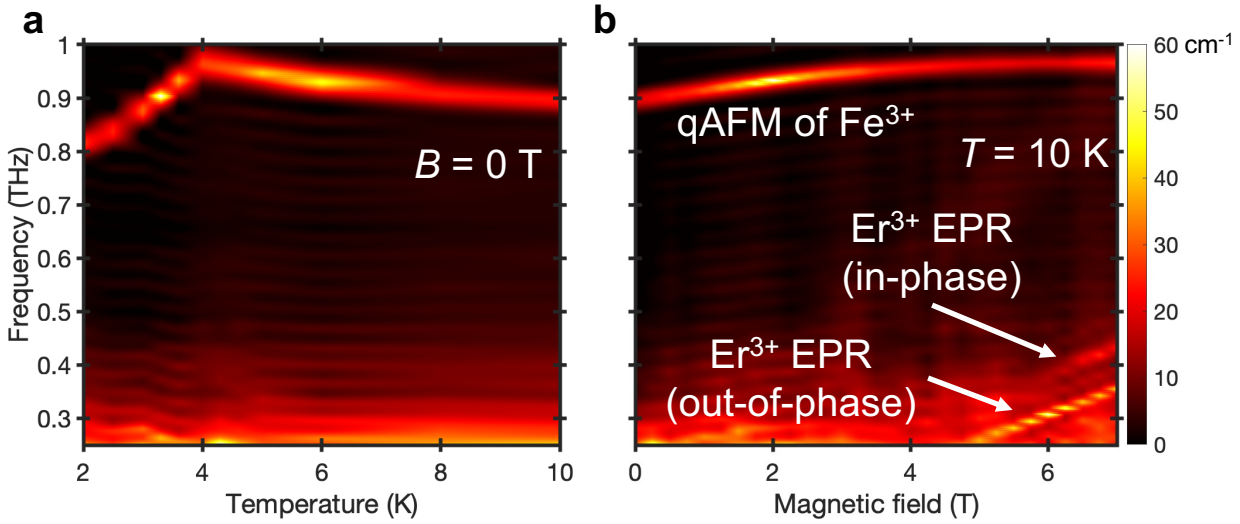

Extended Data Fig. 1. Terahertz absorption coefficient spectra. a, Absorption coefficient spectra as a function of temperature in THz-TDS, showing a kink at the phase boundary. **b**, Absorption coefficient spectra as a function of the magnetic field in THz-TDMS. The qAFM mode of Fe^{3+} and two Er^{3+} EPR modes are observed. Fig. 3b (right panel) plots the out-of-phase mode. Our mean-field calculation in Extended Data Fig. 5c shows all three modes.

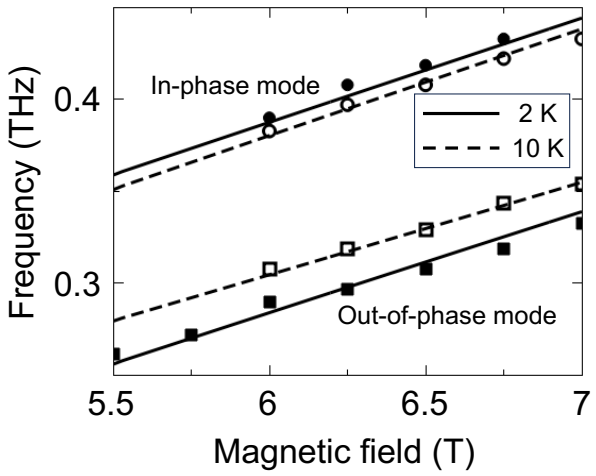

Extended Data Fig. 2. In-phase and out-of-phase modes of Er^{3+} spins below and above the critical temperature, showing shifts only for the 2 K case; Lines (theory), filled points (2 K, experiment) and empty points (10 K, experiment).

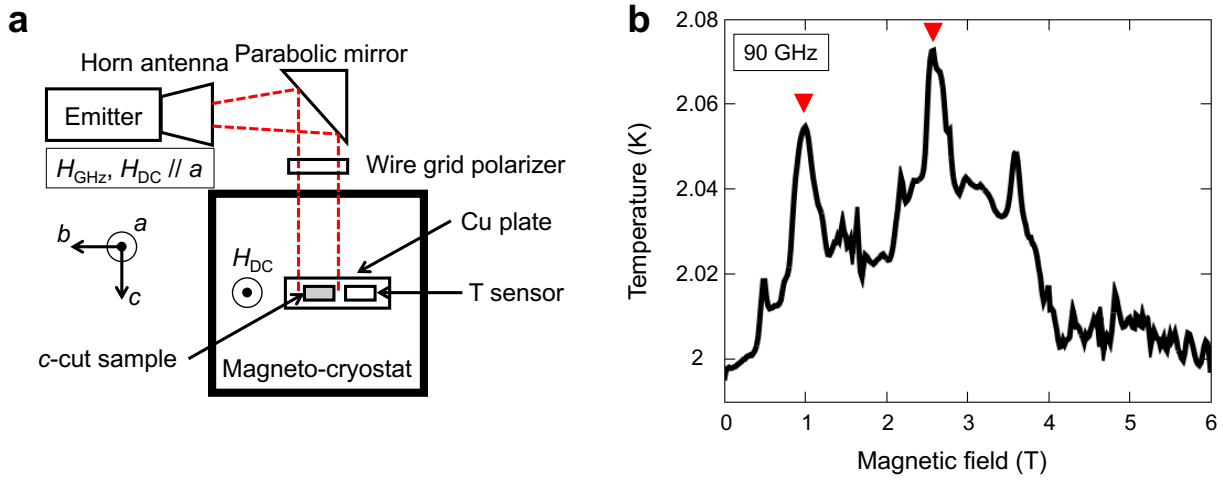

608 **Extended Data Fig. 3. Thermal detection of Er^{3+} EPR modes.** **a**, A schematic of the setup
609 for thermal detection. **b**, The sample temperature as a function of the static magnetic field with
610 90 GHz illumination. The temperature increases when the incident photon energy coincides with
611 the transition energy of magnetic resonances.

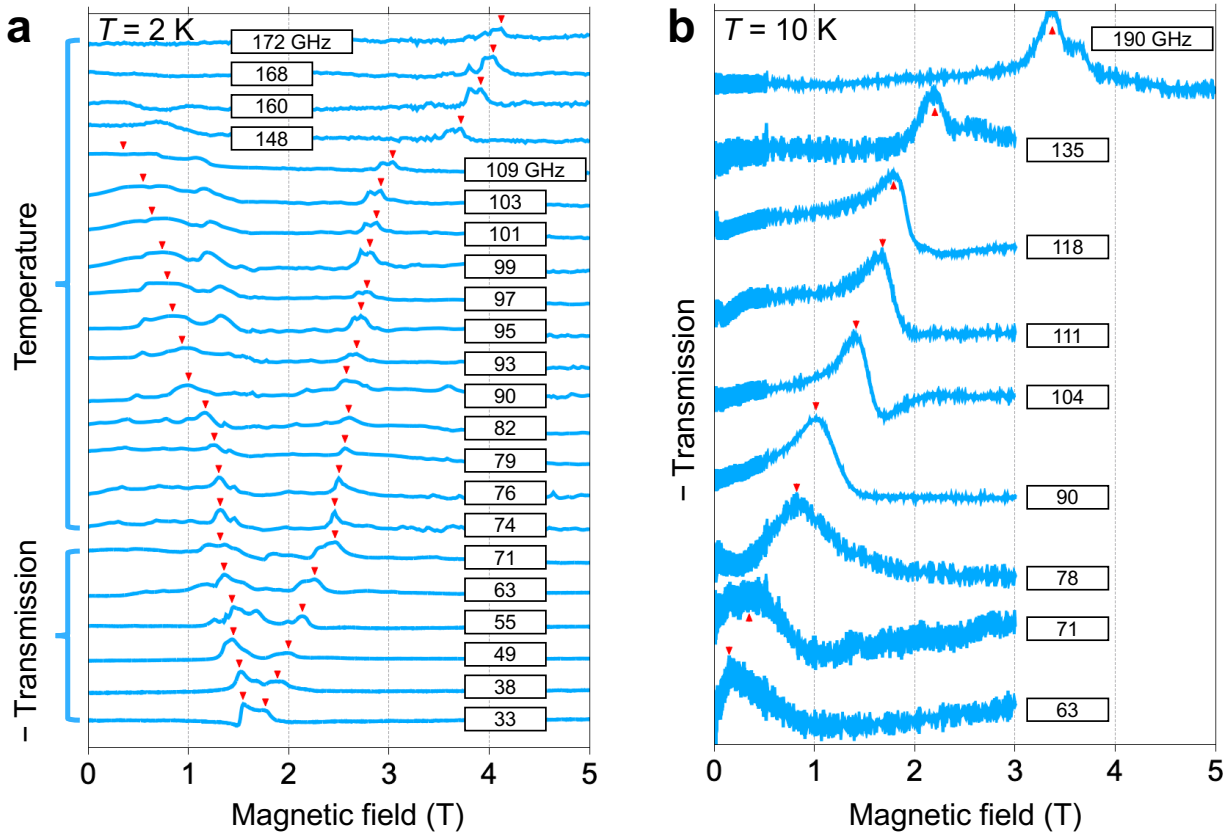

Extended Data Fig. 4. Raw data of GHz measurements with 0-to-1 scale. **a**, From 33 to 71 GHz (74 to 172 GHz), transmission (temperature) spectra as a function of the magnetic field at 2 K. These data are used to generate the two middle and bottom panels in Fig. 2c. **b**, From 63 to 190 GHz, transmission spectra as a function of the magnetic field at 10 K. Red triangles indicate the resonance peak positions in Fig. 3b (right panel, red circles).

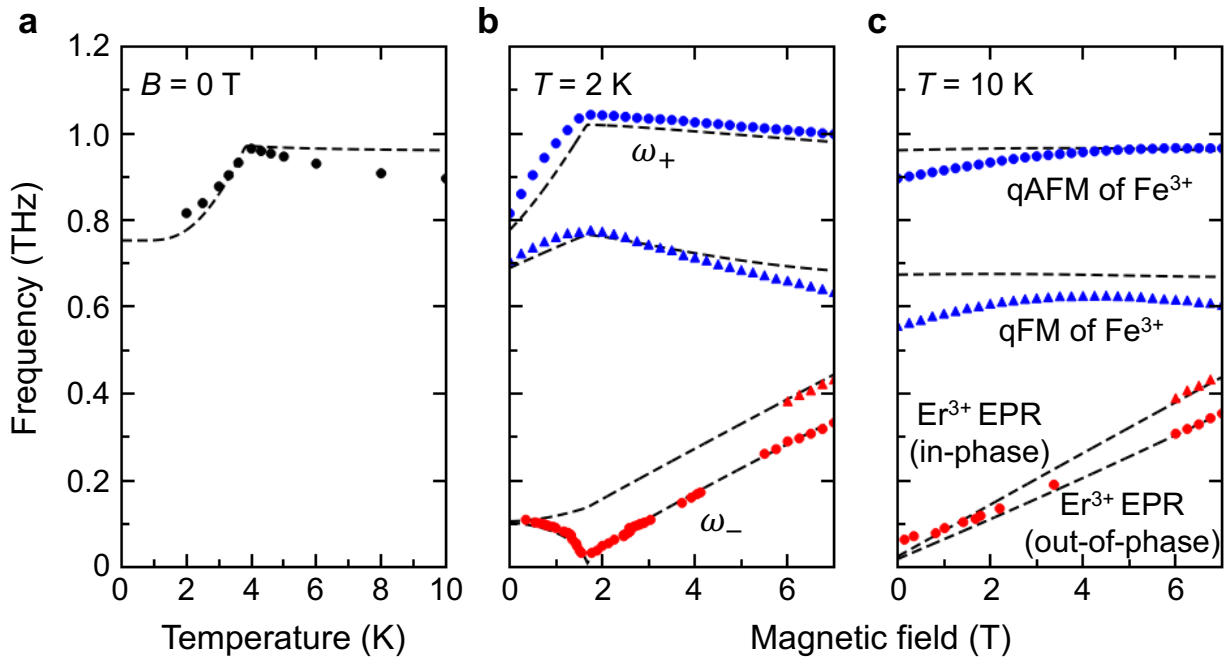

Extended Data Fig. 5. Comparison between experimental data and fitting results. **a**, Temperature dependent absorption peaks of the qAFM mode of Fe^{3+} extracted from Extended Data Fig. 1a. **b, c**, Magnetic field dependent absorption peaks of all four modes at 2 K (**b**) and at 10 K (**c**). We present our fitting curves in (**a**) and (**b**), and calculations for 10 K in **(c)**. The blue circles, red triangles, and red circles in (**b**) are extracted from Fig. 2c, while those in (**c**) are from Extended Data Fig. 1b. The blue triangles correspond to the qFM mode of Fe^{3+}, obtained from separate experiments with a 90° rotated incident THz magnetic field polarization (not shown).

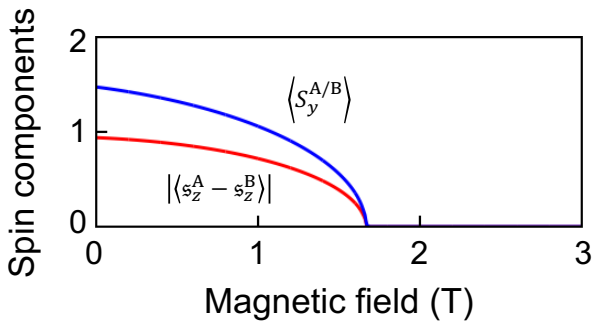

624 **Extended Data Fig. 6.** Two order parameters evidencing the magnonic SRPT calculated at 2 K in

625 the presence of the magnetic field.

Fe^{3+} subsystem	Er^{3+} subsystem	Fe^{3+}–Er^{3+} interaction
$J_{\text{Fe}} = 4.96\,\text{meV}$	$J_{\text{Er}} = 0.01328(5)\,\text{meV}$	$J = 0.6\,\text{meV}$
$D^{y}_{\text{Fe}} = -0.107\,\text{meV}$	$A^{x}_{\text{Er}} = 0.124(4)\,\text{meV}$	$D_x = 0.034\,\text{meV}$
$A^{x}_{\text{Fe}} = 0.0073\,\text{meV}$	$A^{z}_{\text{Er}} = 0.1480(3)\,\text{meV}$	$D_y = 0.003\,\text{meV}$
$A^{z}_{\text{Fe}} = 0.0176(3)\,\text{meV}$	$A^{xz}_{\text{Er}} = 0\,\text{meV}$	
$A^{xz}_{\text{Fe}} = 0\,\text{meV}$	$\mathfrak{g}^{x}_{\text{Er}} = 4.16(8)$	
$\mathfrak{g}^{x}_{\text{Fe}} = 3.5734(3)$	$\mathfrak{g}^{y}_{\text{Er}} = 3.4$	
$\mathfrak{g}^{y}_{\text{Fe}} = 2$	$\mathfrak{g}^{z}_{\text{Er}} = 9.6$	
$\mathfrak{g}^{z}_{\text{Fe}} = 0.6$		

Table 1: Mean field model parameters from fitting and Ref.[5]. Listed parameter uncertainties are errors of fit, determined by the method in Ref.[47].